sustainability

Article

Assessment of Climate Change Impacts for Balancing Transboundary Water Resources Development in the Blue Nile Basin

Mihretab G. Tedla [1,2,*], Mohamed Rasmy [1,2], Katsunori Tamakawa [1], Hemakanth Selvarajah [1,2] and Toshio Koike [1,2]

1 International Centre for Water Hazard and Risk Management under the Auspices of UNESCO (ICHARM) & Public Works Research Institute (PWRI), 1-6 Minamihara, Tsukuba 305-8516, Japan
2 National Graduate Institute for Policy Studies (GRIPS), Roppongi, Minato-ku, Tokyo 106-8677, Japan
* Correspondence: mihretab@icharm.org; Tel.: +81-90-6002-9925

Abstract: An assessment of climate impacts in the hydrologic system of the Blue Nile basin is useful for enhancing water management planning and basin-wide policymaking. Climate change adaptation activities predominantly require an understanding of the range of impacts on the water resource. In this study, we assessed climate change impacts on the Blue Nile River using 30-year in situ climate data (1981–2010) and five bias-corrected General Circulation Models (GCMs) for future (2026–2045) climate projections of RCP8.5. Both historical and GCM precipitation projections show inter-annual and spatial variability, with the most significant increases in the rainy season and a significant decrease in the dry season. The results suggest the probability of an increase in total precipitation. The intensity and frequency of future extreme rainfall events will also increase. Moreover, the hydrological model simulation results show a likely increase in total river flow, peak discharges, flood inundation, and evapotranspiration that will lead to a higher risk of floods and droughts in the future. These results suggest that the operation of water storage systems (e.g., the Grand Ethiopian Renaissance Dam) should be optimized for Disaster Risk Reduction (DRR) and irrigation management in addition to their intended purposes in the Nile basin.

Keywords: climate change; hydrological model; flood and drought; reservoir; Blue Nile basin

check for updates

Citation: Tedla, M.G.; Rasmy, M.; Tamakawa, K.; Selvarajah, H.; Koike, T. Assessment of Climate Change Impacts for Balancing Transboundary Water Resources Development in the Blue Nile Basin. *Sustainability* **2022**, *14*, 15438. https://doi.org/10.3390/su142215438

Academic Editor: Zhenliang Yin

Received: 17 October 2022
Accepted: 14 November 2022
Published: 21 November 2022

1. Introduction

The African region is one of the most vulnerable continents in terms of climate change and climate variability [1]. It is predicted that the direct impacts of climate change on the water–food–energy nexus will pose an increasing number and types of risks to life and livelihood in the African region. Moreover, IPCC AR5 reports that reduced precipitation is likely over North Africa and the southwestern parts of South Africa, while in sub-Saharan Africa, particularly in high or complex-topography regions such as the Ethiopian Highlands, rainfall and extreme rainfall are likely to increase [2]. The rainfall pattern in the tropics is strongly influenced by large-scale features including Hadley Circulation, the pattern of sea surface temperatures, the effects of planetary waves, and the influence of local winds, which also influences the position of the Inter-Tropical Convergence Zone (ITCZ) [3,4].

The Nile River, the world's longest river, occupies nearly 10% of the landmass of the African continent. It has been used since antiquity for domestic purposes, irrigation, and navigation, but large-scale planning and development only began in the late 19th century as set out by Hurst (see [5]). Currently, water infrastructure such as the Grand Ethiopian Renaissance Dam (GERD), with a capacity of 74 billion cubic meters, is being constructed in response to increasing demand for food, energy, drinking water, and navigable waters. As the Nile is a significant water resource for the nations in the region, its sustainability is crucial under global warming.

Climate change, particularly in transboundary rivers, poses a substantial risk, given the different economic, political, and social interests of the riparian countries that require local and international policy arrangements related to water management. There is growing evidence of climate change: Changes such as rainfall reduction over North Africa and the increase in the frequency of extreme events, place additional pressure on water resources and point to the necessity of a clear all-stakeholder consensus on the best use of model projections in the formation of sound water resource management decisions [6].

Assessment of the impact of climate on water resources requires reliable future hydro-meteorological information and simulations of the entire range of flows within a watershed, in order to provide spatial information on various hydrological components for use in evidence-based policymaking. GCMs perform reasonably well at larger spatial scales and in large land mass areas such as Africa but perform poorly at finer spatial and temporal scales. This is especially true of precipitation, which is a crucial element of hydrological analysis [7,8]. Previous studies found substantially less confidence in the magnitude, and even direction, of regional rainfall changes in Africa [9,10]. A number of examinations of climate change in the Blue Nile basin report a much less homogeneous set of changes in precipitation [11–13]. Other studies report clear discrepancies in the projections of precipitation [14,15] and limited findings due to the coarse spatial resolution and the limited number of GCMs used [16]. There is evidence that the projected changes in rainfall in the Blue Nile were dependent on the climate models used and the downscaling method applied [17]. This points to a need for assessments of climate change through the combination of data from historical observation and detailed analysis of climate variables in GCMs. Despite considerable progress, climate model simulations still require further adjustment before they can be applied to climate change impact studies [18,19].

Recent advances in science and technology (e.g., GCM selection and downscaling techniques on GCM's projection performance with in situ data and advances in hydrological models) now enable reliable quantification of the impacts of climate change on water resources and water-related disasters at the basin level. However, not only is the use of regional climate models for the dynamical downscaling of GCMs computationally demanding but also the results are not at a scale suitable for application in hydrological models [20]. Studies applying statistical downscaling in GCMs have identified an empirical relationship between the large-scale climate features simulated by the GCM and the fine-scale climate variables observed in various regions [21–23]. In addition, the elimination of biases in statistical bias correction methods and ground observations could further address the major shortcomings of GCM [24]. The selection of several GCMs that represent the regional climate history reasonably well could reduce uncertainties and could enable the inclusion of an uncertainty assessment in climate change impact studies [25]. The individual analysis of GCM characteristics could promote transparent management of uncertainty, in contrast to multi-model ensemble analysis, where uncertainty can vanish due to the reduction of the confidence interval around the mean [26]. Importantly assessment of the variance in GCM projections increases research objectivity and can enhance impact evaluations and the quality of policy suggestions [27]. In this study, the best-performing GCM on CMIP5 models and bias correction with in situ data were determined using Data Integration and Analysis System (DIAS) [28].

Furthermore, there is a need for physical-based distributed hydrological models (DHMs) with the particular ability to simultaneously address parameters related to floods and drought under the influence of variation in surface energy and temperature to support the evaluation of changes in water availability and hydrological extremes under climate change. Previous studies in the upper Blue Nile basin used semi-distributed models, which constrained parameters within certain ranges that have clear physical meanings [29–31]. The Water–Energy Budget Rainfall-Runoff-Inundation (WEB-RRI) model, which incorporates water and energy budget processes, land–vegetation–atmosphere interactions, multilayer soil moisture dynamics, and inundation processes, was developed and used in simulations of low flow, flood onset timing, and inundation characteristics [8,32]. For those reasons, the WEB-RRI model was selected for the simulation of past and future GCM outputs for Blue Nile projections. Moreover, flow projections are expected to provide information for reservoir management to mitigate significant problems caused by hydrological extremes under climate change.

As climate-related hazards such as floods, storms, and droughts continue to cause major disasters globally, international policies such as the Sendai Framework for Disaster Risk Reduction (SFDRR) have been formulated by global leaders to strengthen the resilience of societies to disasters [33]. The United Nations Framework Convention on Climate Change (UNFCCC) Paris Agreement addressed the topic of water adaptation by adopting a focus on the protection of the ecosystem and biodiversity, so as to enhance environmental resilience to climate change [34]. Equitable and reasonable water utilization in conjunction with the principle of cooperation and obligation against causing significant harm will ensure the development, conservation, and management of international watercourses. In this context, climate change impact assessment and qualitative presentation are essential for the understanding and management of risk; implementation and management of risk; implementation of mitigation measures; and strengthening of adaptation mechanisms, particularly in transboundary river basins.

This study aims to develop a methodology for the assessment of the climate change impact on future water resources of the Blue Nile basin. The range of the projection and analyses conducted in this study is wider than that in previous studies, mainly due to four factors:

(a) The combined use of selected GCMs and 30-year observed data.
(b) Analysis of uncertainty in GCM projections.
(c) The use of a distributed hydrological model with a wide range of simulation capabilities.
(d) The application of qualitative assessment to decision making.

The results of the hydrological extremes projections were also unique representations of the climate change hazards for inputs in disaster risk reduction. The approach adopted here is developed for the evaluation of climate change impact under uncertainty and to guide robust decision-making for development in a transboundary basin. Future directions of this research will focus on reservoir optimization and investigation of water resource management practices under a changing climate to support the facilitation of transboundary water development and cooperation in the Nile basin.

2. Materials and Methods

2.1. Study Area

The Blue Nile (Abbay) is the main tributary to the Nile Basin covering a catchment area of approximately 312,000 km^2 and providing 62% of the flow reaching the Aswan dam [35]. The basin has highly rugged topography and a huge variation of altitude extending from approximately 370 m above sea level (masl) at Khartoum to more than 4220 (masl). More than 50% of the Blue Nile catchment in Ethiopia is within the north-central Ethiopian highland. The river tributaries drainage area also includes Dedesa and Dabus sub-basins and a large proportion of the western and south-western highlands of Ethiopia before dropping to the plains of Sudan. The seasons in Ethiopia are classified into October–January (Bega), February–May (Belgi), and June–September (Kiremt) seasons [36].

2.2. Data

2.2.1. Topographic Data

Topographic data, including digital elevation models, flow direction, and flow accumulation, were obtained from the U.S. Geological Survey (HydroSHEDS) 1 arc-minute (~1800 m) of hydrologically accustomed data, improved from the original DEM by means of procedures including void-filling, filtering, and upscaling. Soil-type distribution data were obtained from the Food and Agriculture Organization (FAO) at a 9 km spatial resolution. The land-use data were collected from United States Geological Survey (USGS) global datasets with a spatial resolution of 1 km and reclassified via the Simple Biosphere Model2

(SiB2) [37]. In this study, Terra satellite's Moderate-Resolution Imaging Spectroradiometer (MODIS) global products (MCD15A2H) of the Fraction of Photosynthetically Active Radiation (FPAR) and Leaf Area Index (LAI) version 6 (based on an 8-day composite dataset with aa 500 m pixel size) were used to produce vegetation phenology inputs for the estimation of surface energy, water, and carbon budget processes in the model.

2.2.2. Temporal Data

The temporal data include observed and reanalysis weather and streamflow data. The higher the temporal resolution of the record, the higher the accuracy of the flow estimation [38]. In this study, the observed daily precipitation data from 12 observation stations and daily minimum and maximum temperatures from nine stations for the period of 1981–2010 were obtained from the Ethiopian National Meteorological Agency. The stations are located upstream of the Blue Nile basin and within the Ethiopian boundary, as shown in Figure 1. Data quality control was performed on the original data and used for analysis. Similarly, observed daily river discharges for 1981–2010 were obtained from the Ministry of Water and Energy at the Abbay near Kessie station at 10.07 latitudes and 38.18 longitudes. Additionally, monthly flow data were obtained for Bahir-Dar, Border (the Ethiopia–Sudan border), and Khartoum stations on the Blue Nile River.

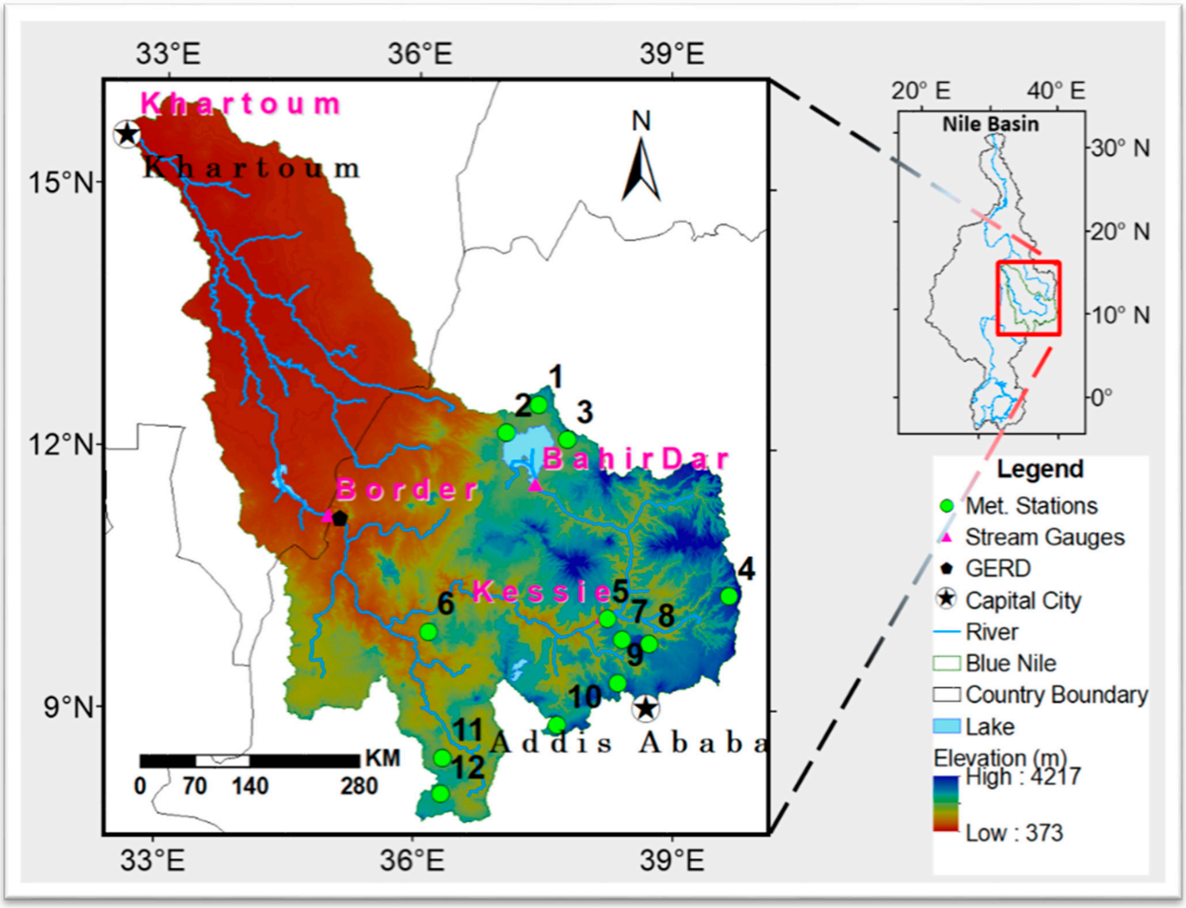

Figure 1. Study area map.

Meteorological forcing inputs were also obtained from the Japanese 55-year Reanalysis (JRA-55) data prepared by the Japan Meteorological Agency (JMA). The JRA-55 data analysis period covers 1958 onwards, making it a high-quality homogeneous re-analysis climate dataset covering the last half-century for the entire globe [39]. The JRA-55 data are available at a 3 h temporal resolution and 0.125° spatial resolutions for air temperature, wind speed, specific humidity, and surface pressure, and 0.56° spatial resolutions for downward radiations. These data were interpolated to model grid resolutions of ~1800 m using a linear interpolation method in the WEB-RRI model.

2.3. Methods

The research design consists of three main components: (a) Climate change trend assessment on observations and GCMs climatic variables (i.e., temperature and precipitation); (b) analysis of local- and synoptic-scale climate variables in GCMs for understanding the projection uncertainties; (c) hydrological model development using WEB-RRI for baseline (1981–2000) and future (2026–2045) periods for the estimation of the water balance and extreme flows along the river, including future inflow changes at the Great Ethiopian Renaissance Dam (GERD). The overall methodological flow of the study is shown in Figure 2 below.

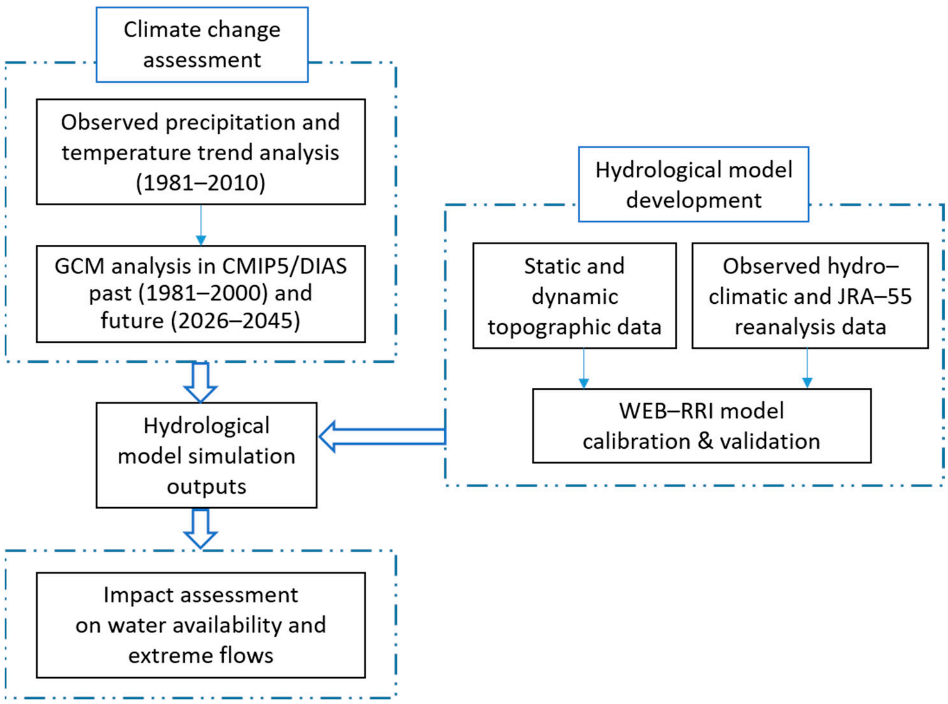

Figure 2. Methodological flow chart of the study.

2.3.1. Monotonic Trend Analysis

Parametric and non-parametric tests are commonly used in trend analysis of time series such as hydro-climatic data. In this study, non-parametric trend analysis in precipitation time series was applied using the Mann–Kendall test for trends [40,41] and Sen's slope estimator [42]. Non-parametric trend tests require only that the data be independent and flexible to outliers in the data [43]. Additionally, techniques that do not require assumptions about the data distribution, such as rank techniques and percentage changes, have been used in trend assessment. Deviations from the mean were used to assess the trend in temperatures in long-term observation data. Wet and dry spells were also classified based on the basin's average consecutive wet, dry, no-rain, and high-rain records.

2.3.2. Meteorological Assessment from GCM

The CMIP5 tool function in DIAS enables a 2-D comparison of the model output with reference data and was used to select GCMs for examination of the study area by applying seven meteorological elements: Precipitation, air temperature, outgoing longwave radiation, sea-level pressure, zonal wind, meridional wind, and sea-surface temperature. The long-term average values of an inspected element for a particular month with respect to climatology and the grid-by-grid model output vs. reference data were used to calculate the spatial correlation coefficient (Scorr) and Root Mean Square Error (RMSE) [28]. In the selection of GCMs, the RMSE and Scorr values of all models were averaged over the evaluation period. Index (1, 0, −1) based on the RMSE and Scorr of each model were assigned and then summed for all inspected elements to provide a ranking for each model. The models with the highest rank will be used in the generation of future rainfall. The GCM selection is crucial due to the huge storage requirement and insufficient utilization of the models.

In this study, five GCMs were selected among the 44 models available in DIAS-CMIP5 based on regional performance: MPI-ESM-LR and MPI-ESM-MR (both from Germany), ACCESS1.0 (Australia), CESM1(CAM5) (USA), and CMCC-CMS (Italy). The selected GCMs were subjected to bias correction with observed data. A three-step statistical bias correction method was applied to precipitation: (a) Generalized Pareto distribution for extreme rainfall correction; (b) gamma distribution for normal-rainfall correction; and (c) statistical ranking order for no-rain day correction incorporated into the DIAS-CMIP5 tool [24]. The bias-corrected rainfall data were spatially distributed using the Thiessen polygon method to force the hydrologic model simulation. Though some countries around the world made efforts to reduce GHG emissions, the IPCC AR6 reports indicate the annual average emission in 2019 was approximately 12% higher than in 2009 and 54% higher than in 1990. The annual average during the decade of 2010–2019 was the highest decadal emissions increase on record from 2000–2009 [44]. Consequently, climate change evaluation with the RCP 8.5 "Business as usual scenario" was performed to evaluate the worst-case climate change impact on the climatic parameters and water resources of the Blue Nile basin.

2.3.3. Discharge Simulation

To evaluate the hydrological variables, a physical-based distributed model (DHM) and the Water Energy Budget-based Rainfall-Runoff-Inundation model (WEB-RRI) were developed and validated with observed discharge data. WEB-RRI is structured into four major modules: (1) The Simple Biosphere Model 2 (SiB2) module for the vertical energy and water flux transfer between land and atmosphere for each model grid; (2) the vertical soil moisture distribution module based on Richard's equation and Darcy's equations for groundwater recharge; (3) the 2-D diffusive wave lateral flow module for surface flow and groundwater flow; and (4) the 1-D diffusive wave river flow module. The model implemented the connections between surface and river and groundwater flow, and soil moisture content and groundwater and river discharge [45]. The WEB-RRI model incorporates the simulation of wide-ranging hydrologic elements and he evaluation of water and energy fluxes.

2.3.4. Evaluation Indices

Hydrologic model parameters must be derived from the calibration using one or more observed variables with modelled results, e.g., streamflow. The comparison indices provide physical meaning and adequate ranges for their values. The evaluation of the model performance has been tested using statistical measures including the Nash–Sutcliffe equation (*NSE*), Mean Bias Error (*MBE*), and Root-Mean-Squared Error (*RMSE*) for model performance (i.e., the strengths and weaknesses of the model). This measures-oriented method to model performance evaluation takes into account several different aspects of the model's correctness or skill. The equations for testing are shown below:

$$NSE = 1 - \left[\sum_{i=1}^{n} (O_i - S_i)^2 / \sum_{i=1}^{n} (O_i - \overline{O})^2 \right], \tag{1}$$

$$MBE = \sum_{i=1}^{n} (O_i - \overline{O}) / n \tag{2}$$

$$RMSE = \sqrt{\sum_{i=1}^{n} (O_i - S_i)^2 / n}, \quad (3)$$

where O_i is the measured values of flow (m^3/s), S_i is the simulated values, $\overline{O}$ is the mean measured values, and n is the number of data points.

2.3.5. Qualitative Assessment

Decision-making regarding climate change policy, particularly in transboundary basins, is a very complex and demanding task since there is no single decision maker and different stakeholders tend to assign different values to climate change impacts. IPCC AR5 and AR6 developed a framework for applying expert judgment in the evaluation of the findings and communication of the state of knowledge [32]. In IPCC-AR6, five qualifiers have been used to classify climate change: Very low, low, medium, high, and very high. In this study, qualitative indices were used to classify climate change evaluations for ease of decision-making. Therefore, if all five GCMs agree, the trend is classified as extremely likely. If the four models agree, it is very likely. If three models, including high-ranking models, agree, it is classified as likely; otherwise, it is classified as uncertain. The water availability and extremes at various locations were also evaluated in the same manner.

3. Results

3.1. Meteorological Assessment

3.1.1. Temperature

Seasonal and annual trends of daily mean temperature between 1981 and 2010 were examined in terms of the deviation from the mean temperature, as shown in Figure 3. In the Bega (ONDJ) season, the average temperature increased slightly by 0.3 °C during the observation period (Figure 3a). In the Belgi (FMAM) season (Figure 3b), the deviation increased by 1.2 °C, while in the Kiremt (JJAS) season (Figure 3c), temperature deviation increased by 0.8 °C, indicating variability in the changes between seasons. The annual average temperature was observed to be monotonically increasing up to 0.7 °C over the analysis period (Figure 3d).

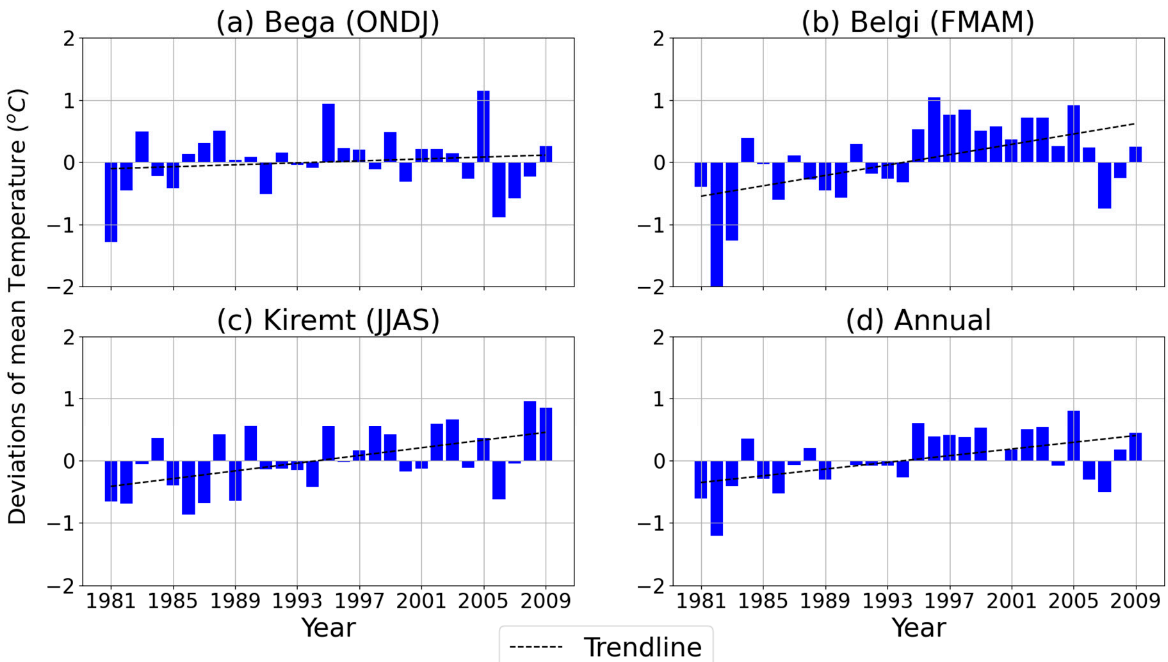

Figure 3. The deviations of seasonal and annual average temperature from the climate norm (1981–2010).

The temperature difference in GCM between the past (1981–2000) and predicted temperatures (2026–2045) suggests that there will be an average increase ranging between 1 °C and 2.5 °C for all selected models, as shown in Figure 4. The temperature increases for all seasons with marginal variation among months, indicating a high likely temperature increase in the future period. Those temperature differences were also used to correct the JRA-55 air temperature for future hydrologic model simulations.

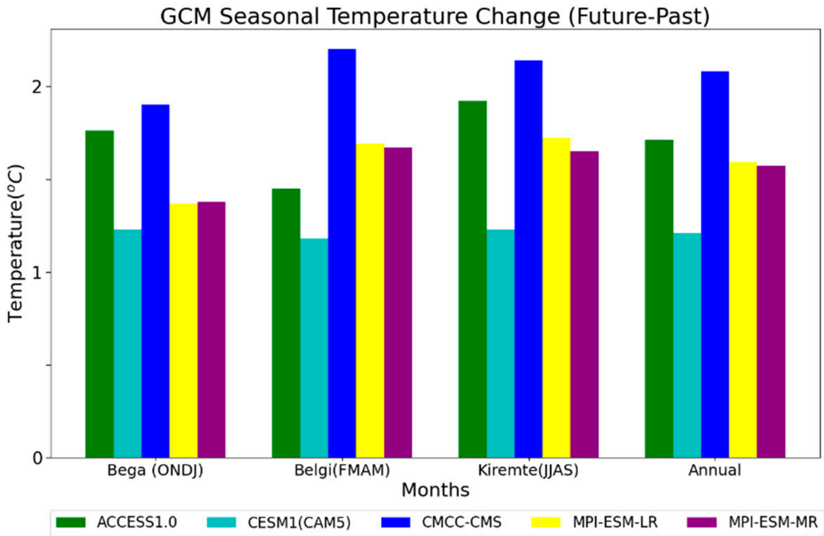

Figure 4. GCM temperature differences in the future (2026–2045) and past (1981–2000).

3.1.2. Extreme Precipitation

Climate change in terms of climatic extreme dry and wet conditions was estimated from the observed data as shown in Figure 5. A basin average precipitation threshold for no rain days and high rainfall was selected to accommodate the variability in the rainfall record between the observation stations. The consecutive dry days (CDD) trend indicates a monotonic increase over the observation period, as shown in Figure 5a. Similarly, consecutive wet days (CWD) indicate an increasing trend as shown in Figure 5b. Further, extreme events with the count of days that recorded a basin average rainfall of less than 1 mm/day (Figure 5c) and above 10 mm/day (Figure 5d) show increasing trends in both extremes. A high number of consecutive and total wet days correlate with overland flooding due to land saturation and flow concentration in catchments, while an increase in the number of consecutive dry days positively correlates to a drought frequency increase due to high evapotranspiration and soil water stress.

Similarly, a comparison of extreme events with the peak recorded rainfall from past and future GCMs were ranked as shown in Figure 6. All GCMs indicate higher peak rainfall intensity in the future projection. As a result, the occurrence of extreme climate events in the Blue Nile basin will high likely increase in the future period. These also echo the increase in the frequency of flash and riverine floods observed in the downstream area of the Blue Nile basin in the recent past, particularly in 2020 and 2021. Changes in extreme weather and climate events, including an increase in the number of heavy precipitation events in several regions, have been linked to human influence [46].

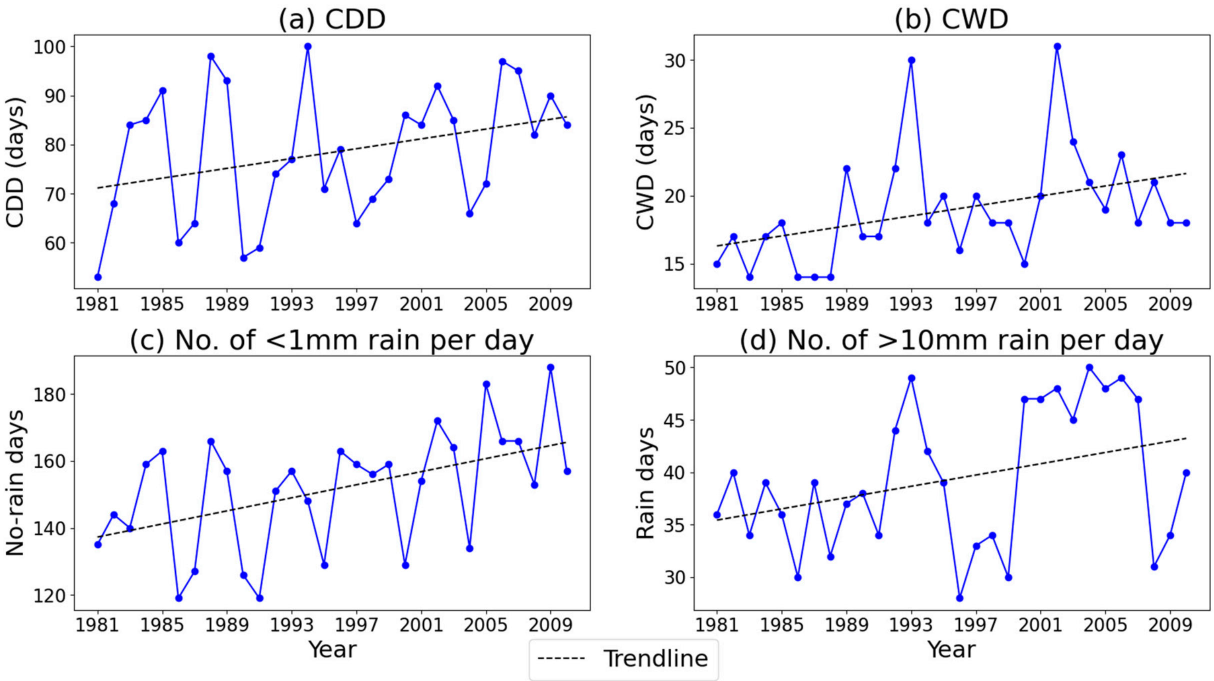

Figure 5. Annual time series and trends in annual extreme climatic conditions, showing (**a**) Consecutive Dry Days (CDD); (**b**) Consecutive Wet Days (CWD); (**c**) days recording less than 1 mm/day; and (**d**) days recording more than 10 mm/day.

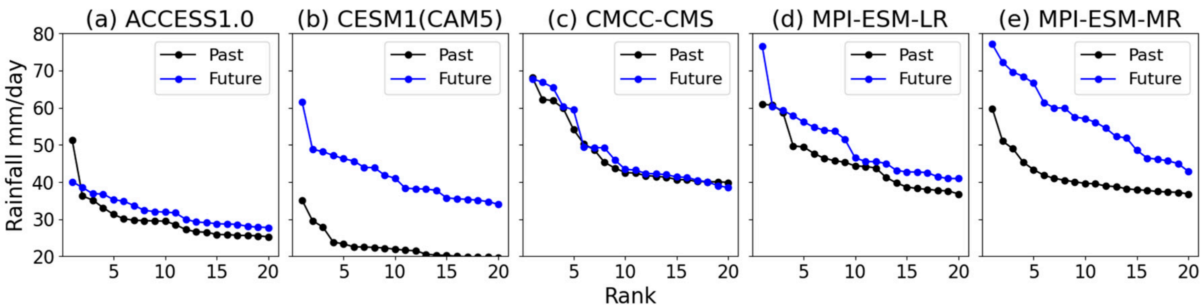

Figure 6. Peak rainfall rank for GCMs.

3.1.3. Total Precipitation

Precipitation in the observation data between 1981 and 2010 was analyzed using a non-parametric evaluation at each observation station considering the Mann–Kendall and Sen's slope tests. From the results, both increasing and decreasing trends were observed over different seasons. As can be noted from Table 1, in the Kiremt season, 9 of 12 stations indicate a significant trend in at least one month between June and September. Decreasing trends in February were observed in five stations located in the central part of the basin. In addition to the spatial and inter-annual difference in increasing and decreasing trends, overall, the basin's total annual trend tends to be increasing at a non-significant level.

Precipitation comparison for GCM past and future indicates higher rainfall in the future period for CESM1(CAM5), MPI-ESM-MR, and MPI-ESM-LR models with 10.9%, +10.7%, and 7.1% increases, respectively. The ACCESS1.0 model indicates negligible or no change (0%), while the CMCC-CMS model projected a decrease of 9.0%, a percentage calculated by (Future − Past)/Past × 100, as shown in Figure 7a. Further, the projected changes in GCM assessed by season (Figure 7b) indicate a significant average precipitation increase for MPI-ESM-LR, MPI-ESM-MR, and CESM1 (CAM5) during the wet Kiremt (JJAS) season. In Bega (ONDJ), only CESM1 (CAM5) predicted a decrease, while in the

Belgi (FMAM) season, four models indicate decreasing trends. The projected changes in precipitation indicated high inter-annual variability.

Table 1. Non-parametric monthly precipitation trend test at observation stations.

	Test	Jan	Feb	Mar	Apr	May	Jun	Jul	Aug	Sep	Oct	Nov	Dec
Gondar	MK (Z)	0	−0.41	0	−0.11	0.62	1.13	1.64	**2.2**	1.24	−0.33	−0.68	−0.17
	Sen's (Q)	0	0	0	−0.08	1.3	3.11	3.1	**4.54**	1.33	−0.78	−0.14	0
Delgi	MK (Z)	0.4	−0.46	0.2	−0.18	0.32	1.23	1.74	**1.6**	1.2	−0.43	−0.82	−0.07
	Sen's (Q)	0	0	0	−0.18	1.2	2.11	2.1	**3.7**	1.1	−0.58	−0.24	0
Addis zemen	MK (Z)	1.25	−0.31	0.18	0.28	0.96	**1.86**	0.45	0.73	1.35	−1.75	0	**−1.81**
	Sen's (Q)	0	0	0	0.1	1.65	**5.61**	3.14	1.73	4.04	−1.77	0	**−1.82**
Mehal_meda	MK (Z)	1.34	**−2.1**	−0.17	−0.99	0.28	1.35	0.67	−0.96	0.34	−1.41	1.48	−0.29
	Sen's (Q)	0.5	**−2.94**	−0.48	−1.15	0.26	1.43	2.49	−1.79	0.48	−0.53	0	0
Filiklik	MK (Z)	−0.71	1.45	−1.21	−0.93	0.39	**2.43**	1.07	0.06	−0.17	−0.59	1.53	−1.08
	Sen's (Q)	0	−0.46	−1.43	−1.11	0.68	**6.8**	4.3	0.45	−0.93	−0.72	0	0
Uka	MK (Z)	−1.19	−0.4	−0.99	−0.17	−0.68	−0.51	1.02	−1.3	0.39	−0.73	−0.51	−0.4
	Sen's (Q)	−0.51	−0.09	−1.03	−0.38	−3.16	−1.53	2.86	−3.77	1.95	−2.15	−0.62	−0.06
Gebrguracha	MK (Z)	0.45	−0.4	−0.03	−0.31	0.85	**2.26**	0.79	−0.85	0	0.4	1.05	−0.15
	Sen's (Q)	0.1	0	0	−0.32	1.79	**4.95**	1.96	−1.77	0.17	0.06	0.01	0
Fiche	MK (Z)	0.99	**−2.03**	−0.9	−0.87	0.62	**2.03**	1.35	−0.23	−0.9	−0.08	**1.8**	−0.55
	Sen's (Q)	0.15	**−2.35**	−0.78	−1.4	0.65	**2.2**	4.79	−0.53	−1.11	−0.03	**0.18**	0
Enchini	MK (Z)	−0.37	**−2.28**	0.34	−0.23	1.24	**1.64**	0.28	0.11	0.06	−0.68	0.85	−0.45
	Sen's (Q)	−0.28	**−2**	0.68	−0.3	3.1	**2.75**	1.03	0.18	0.14	−0.95	0.24	−0.13
Tikurenchini	MK (Z)	0.2	**−2.54**	−0.28	1.41	0.85	1.52	0.62	−0.45	**1.97**	0.68	0.17	−1
	Sen's (Q)	0.11	**−2.33**	−0.89	5.5	1.86	3.8	1.14	−1.35	**5.44**	1.42	0	−0.47
Bedele	MK (Z)	−0.87	−1.13	−1.13	0.23	0.79	**1.69**	**1.69**	1.24	0.85	−0.28	0.93	−0.79
	Sen's (Q)	−0.32	−0.6	−1.2	0.18	2.52	**4.37**	**4.75**	−2.46	2.35	−0.97	1.22	−0.35
Setema	MK (Z)	−0.11	**−1.75**	−1.52	0.68	1.33	−1.18	1.13	−1.07	0	−0.39	−1.18	−1.38
	Sen's (Q)	−0.18	**−1.9**	−2.3	1.2	4.13	−2.81	3.3	−2.45	0.06	−1.57	−0.99	−0.69

Bold is significant at 10%.

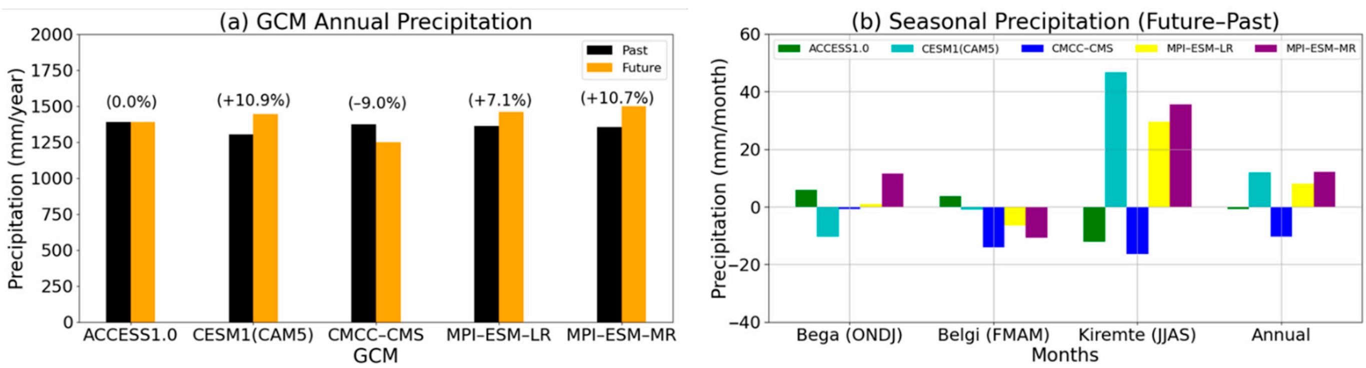

Figure 7. Precipitation changes in GCM between future (2026–2045) and past (1981–2000) (**a**) annual total precipitation (**b**) seasonal precipitation difference.

The spatial distribution of annual precipitation change in GCMs is displayed in Figure 8. Both increasing and decreasing rainfall projections from GCMs were found to be higher in the southern part of the Blue Nile basin. In this study, precipitation estimates from observation data and GCMs indicated that future total precipitation will likely increase, with an increase in basin average precipitation during wet seasons and a decrease in dry seasons. Generally, the results of both observed trends and GCM projection indicate high spatial and intra-annual variability in future precipitation in the Blue Nile basin.

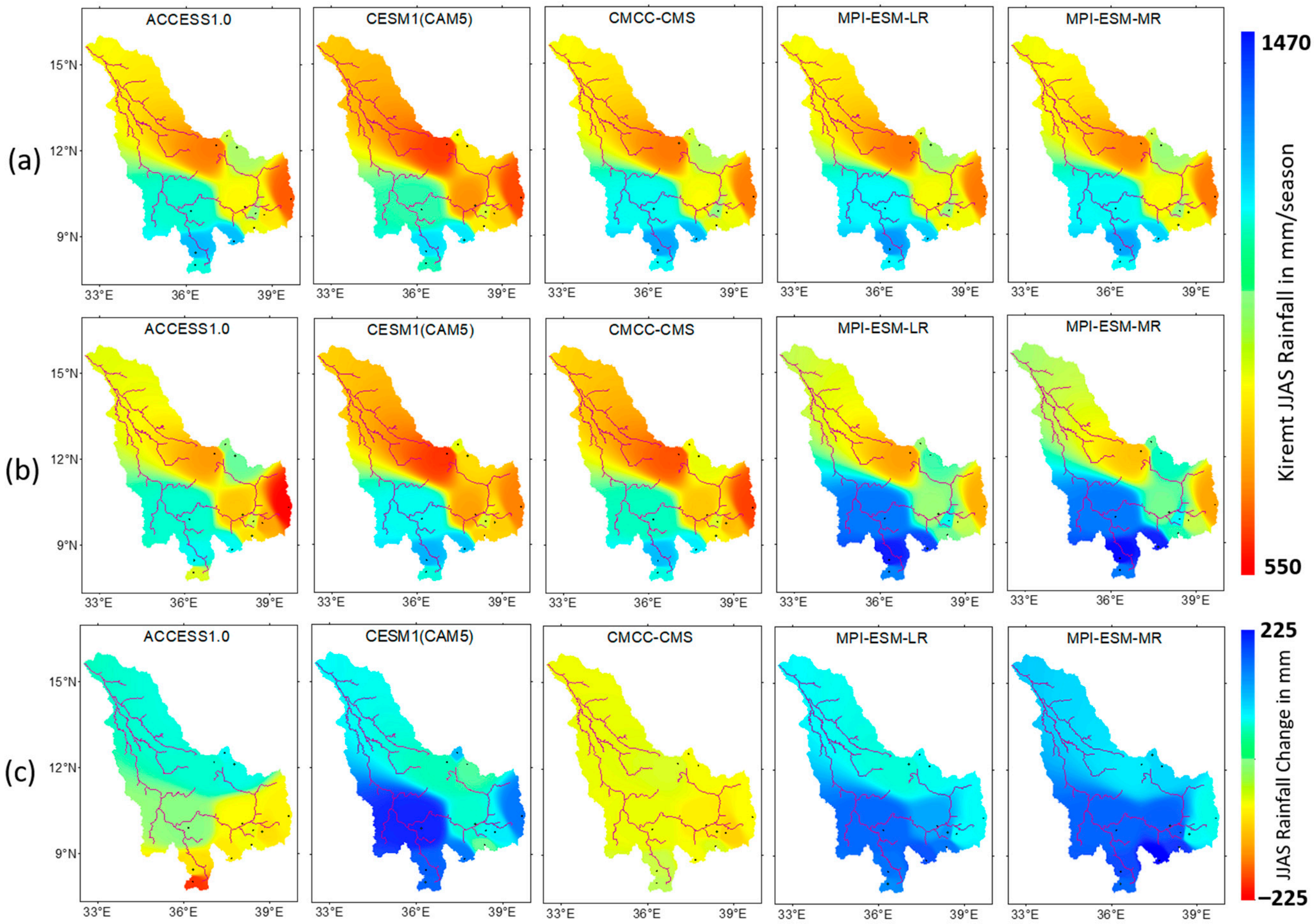

Figure 8. Spatial distribution of JJAS (Kiremt) rainfall for (**a**) past and (**b**) future and (**c**) the change.

3.2. Uncertainty Analysis

In this study, major climatic physical variables over a wider domain were examined using the DIAS-CMIP5 tools to understand the differences in GCM precipitation projections. Variance among GCM projections results from differences in the model formulation and internal variability of climate systems [47]. Various climatic variables' uncertainty on a wider scale and different pressure levels were analyzed statistically and graphically. However, wind speed and direction differences for the Kiremt (JJAS) season were found to linearly correlate with the precipitation projection direction of the GCM models. ACCESS1.0 and CMCC-CMS show strong wind at the southern part of the Indian Ocean diverted towards the southern part of the ocean, with the red region displayed in Figure 9a,c. Wind vectors for CESM1 (CAM5), MPI-ESM-LR, and MPI-ESM-MR models show stronger wind vectors in the southern part of the Indian Ocean directed towards the study area, shown as the purple region in Figure 9b,d,e. These patterns are suggestive of a strong impact of the Indian summer monsoon on the projected rainfall increase, while diverted winds are linked to the decrease in projected precipitation in the Blue Nile basin.

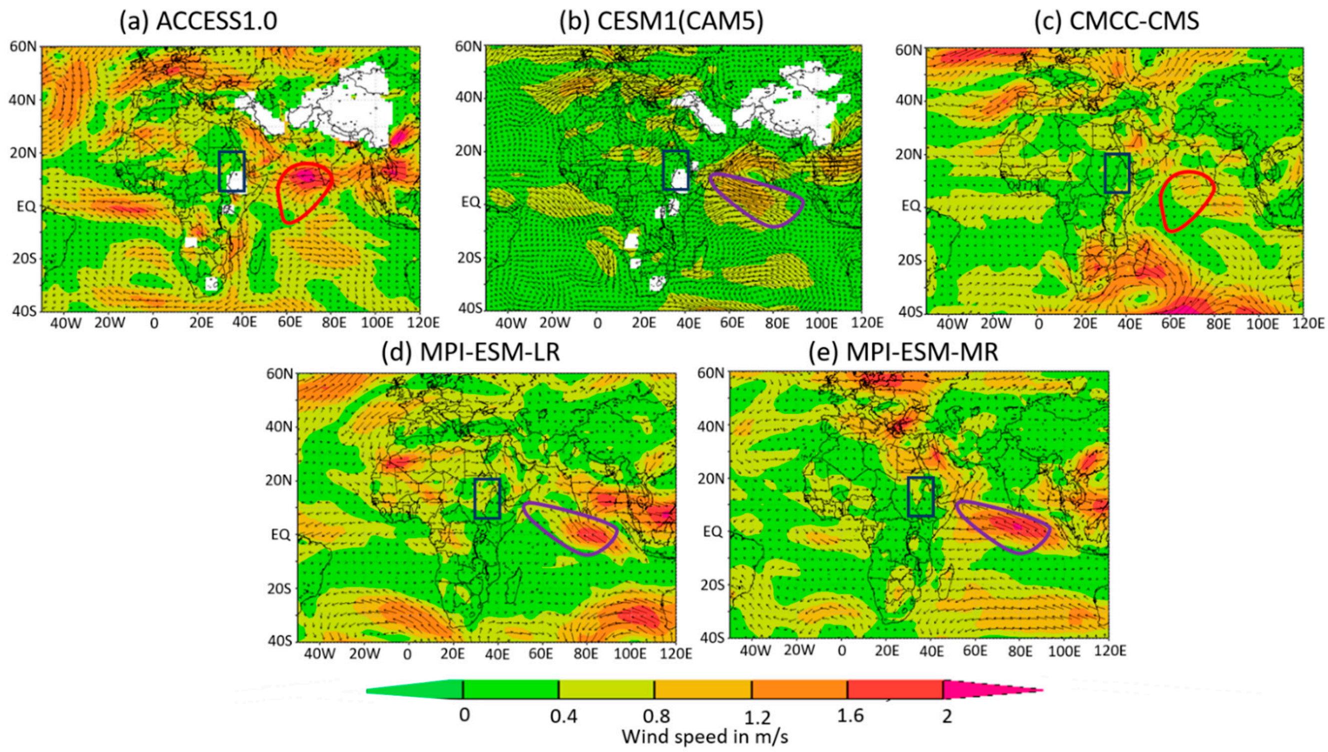

Figure 9. Wind vectors and speed (m/s) differences between future (2026–2045) and past (1981–2000) at 850 hPa pressure level in the Blue Nile basin.

Furthermore, the movement of the ITCZ in response to the position of the sun and tread winds is responsible for the convergence and rising of warm, moist air masses into the atmosphere followed by condensation and cloud formation, which create high precipitative storms in tropical latitudes. In most global climate models, more energy flux and cloud bias are responsible for excessive rainfall projections [48]. Lau and Kim [4] found a strengthening of the Hadley circulation and its connection to increased global dryness. This study identifies a linkage between rainfall projections and wind vector movement as well as the south–north difference in the spatial distribution of precipitation change. Analysis of the climate variables differences in GCMs in association with the ITCZ and the Hadley Circulation movement enhances the efficacy of climate models.

3.3. Hydrological Assessment

Calibration and validation of the WEB-RRI model were performed against the observed data at the Abbay Kessie observation station. Calibration was conducted for daily data between 1993 and 1996. The validation is performed for the past simulation period between 1981 and 2000. An acceptable range of error metrics was obtained for both the calibration and validation and matching hydrographs as shown in Figure 10 below.

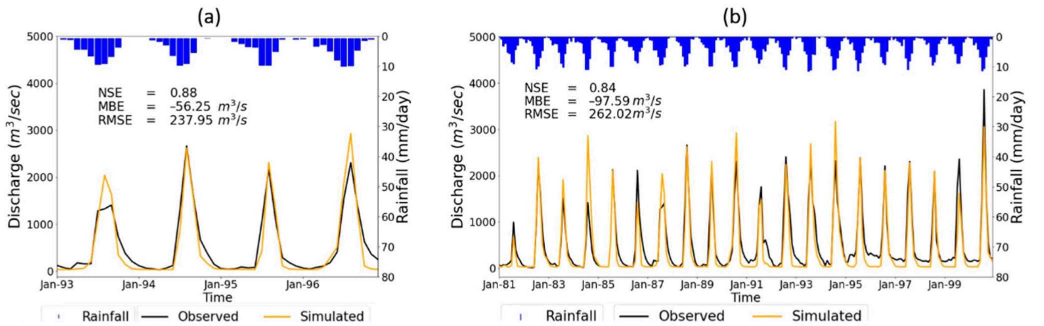

Figure 10. WEB-RRI model (**a**) calibration and (**b**) validation hydrographs.

3.3.1. Water Balance

Hydrologic simulation for each selected model was evaluated with observed discharge data at Abbay Kessie station to assess the GCMs' flow simulation performance in the past. The evaluation results have shown a satisfactory simulation with most of the GCMs attaining an acceptable range for error indices, as shown in Table 2. This evaluation established the model reliability for future discharge prediction based on the past simulation performance.

Table 2. Error metrics for observed and GCMs' past simulation at Abbay Kessie station.

Parameter	Observed	ACCESS 1.0	CESM1 (CAM5)	CMCC-CMS	MPI-ESM-LR	MPI-ESM-MR
NSE	0.84	0.66	0.44	0.58	0.72	0.72
MBE (m^3/s)	−97.59	−126.78	−184.44	−127.28	−97.14	−127.73
RMSE (m^3/s)	262.02	383.91	491.53	425.57	348.02	347.36

The future water balance and its differences from the past at major points along the river have been assessed, as shown in Table 3. The flow in three models indicated increasing total volume while two models showed decreasing values. CESM1(CAM5), MPI-ESM-LR, and MPI-ESM-MR models show an increase in total volume in the future period while CMCC-CMS and ACCESS1.0 models indicate a decrease at all locations from the upstream Lake Tana outlet to the very downstream location at Khartoum. At the border station, which is the inflow to the GERD dam, the projected flow indicated the highest sensitivity to both increases and decreases in the river flow change, while the upstream area was found to show less sensitivity to changes. Thus, the flow projection indicates a likely increase in the total flow in the future period along the Blue Nile River with spatial variability.

Table 3. Annual water balance variability along the Blue Nile River.

Location	GCM Annual Flow Difference in % (Future − Past/Past × 100)				
	ACCESS 1.0	CESM1 (CAM5)	CMCC-CMS	MPI-ESM-LR	MPI-ESM-MR
Bahir-Dar	−5.3	0.5	−24.0	3.6	20.4
Kessie	−10.3	5.6	−26.7	7.5	15.8
Sudan Border	−15.1	11.5	−33.3	8.9	18.3
Khartoum	−6.1	9.7	−25.7	5.2	16.3

On the other hand, evapotranspiration (ET) is projected to increase in all GCMs with annual and seasonal variability, with the highest being in the Kiremt season and the lowest in the Belgi season, as shown in Figure 11. Furthermore, the ET temporal variability reflects the high vegetation transpiration during and after the rainy season. The spatial and temporal distribution of ET in the Blue Nile basin exceeds the potential ET in the period of

May through November [49]. The changes in ET are mainly attributable to the temperature increase incorporated into the future hydrologic model simulation.

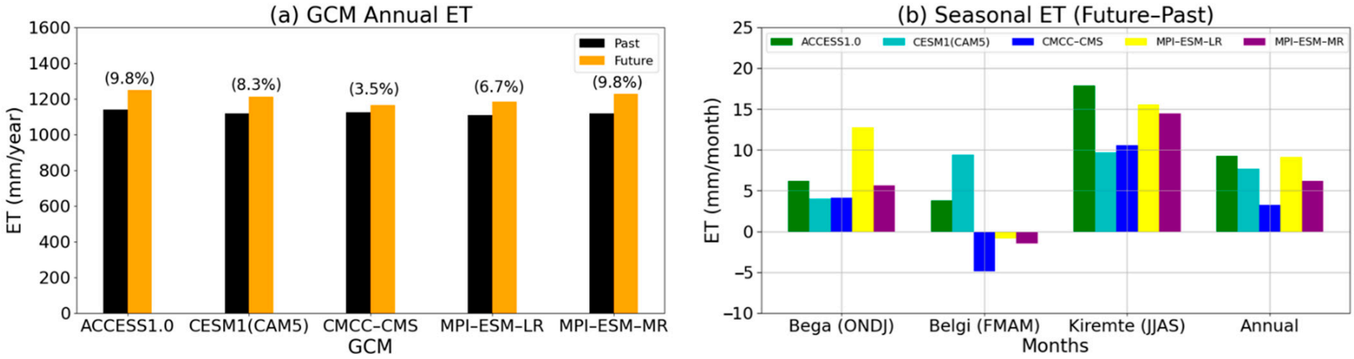

Figure 11. ET changes in GCMs' past and future (**a**) annual differences and (**b**) seasonal differences.

3.3.2. Hydrological Extremes

All-time-high flood inundation maps for the past, future, and difference (future–past) simulations extracted in the WEB-RRI model (Figure 12) indicate an increase in all GCMs. The future inundation area for ACCESS1.0, CESM1(CAM5), CMCC-CMS, MPI-ESM-LR, and MPI-ESM-MR will increase by 2208, 14782, 2618, 753, and 1838 km^2, respectively. In the Blue Nile basin, extreme high flows practically trigger floods around Lake Tana and downstream areas. Typically, the inundation area was identified in the downstream area for both the past and future. Nevertheless, flood control in dams can substantially mitigate disastrous floods in the future period.

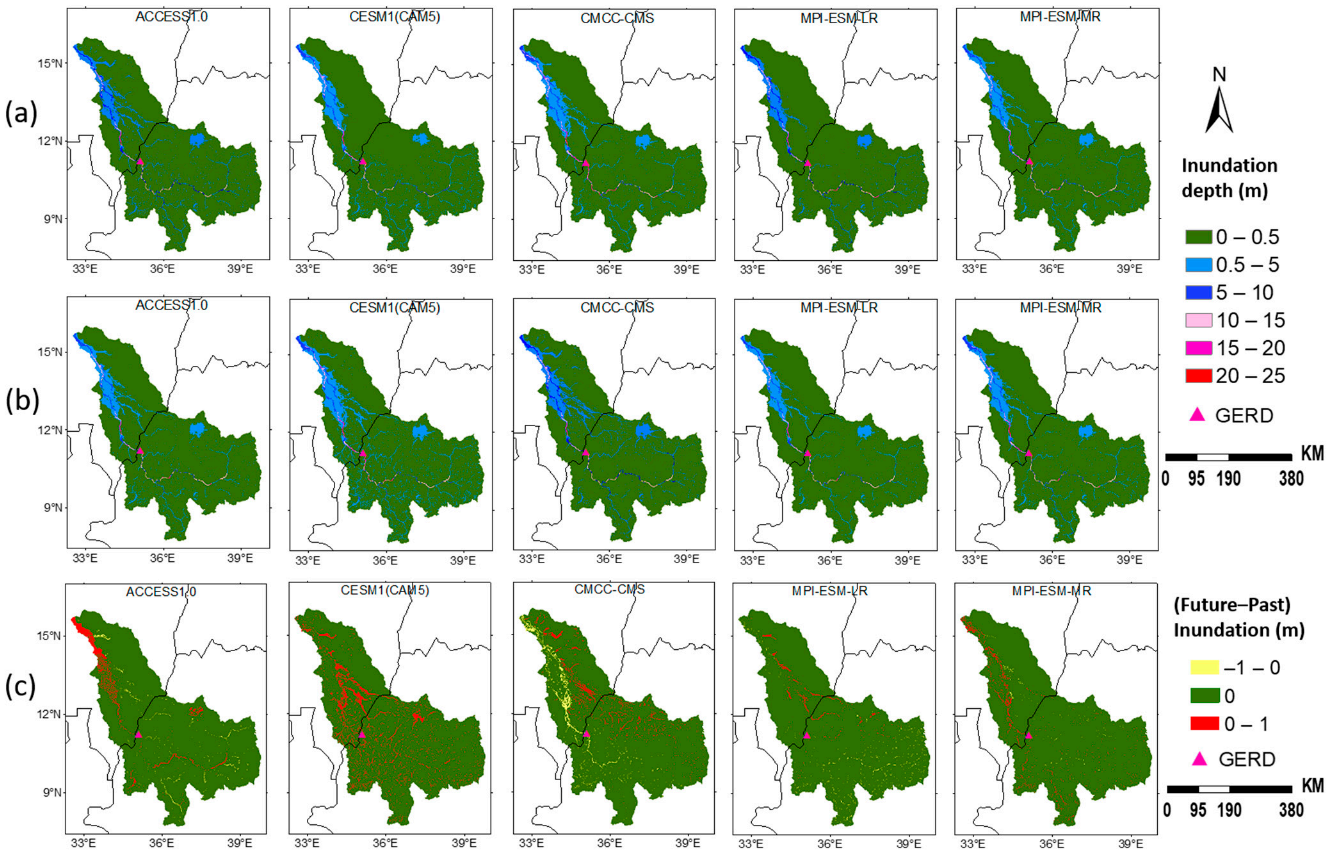

Figure 12. All-time-high flood inundation map of GCMs' simulations: (**a**) Past, (**b**) future, and (**c**) differences between future and past.

Consequently, this study assessed the extreme inflows to the GERD dam to evaluate its potential to control flood flow to the downstream area. The result indicates a likely decrease in extreme low inflow and an increase in extreme high flows, signaling an increase in the frequency of both extreme flows in the future period. Extreme inflows to the GERD dam and the applicability of the dam for flood control against annual maximum and minimum records with real-time flow monitoring are ideal to mitigate the occurrence of disasters. Adjusting the dam operation for hydropower operation of the dam maximizes the benefits to all. The annual total projected inflow to the GERD dam also indicates a likely increase, as shown in the box and whisker graph in Figure 13.

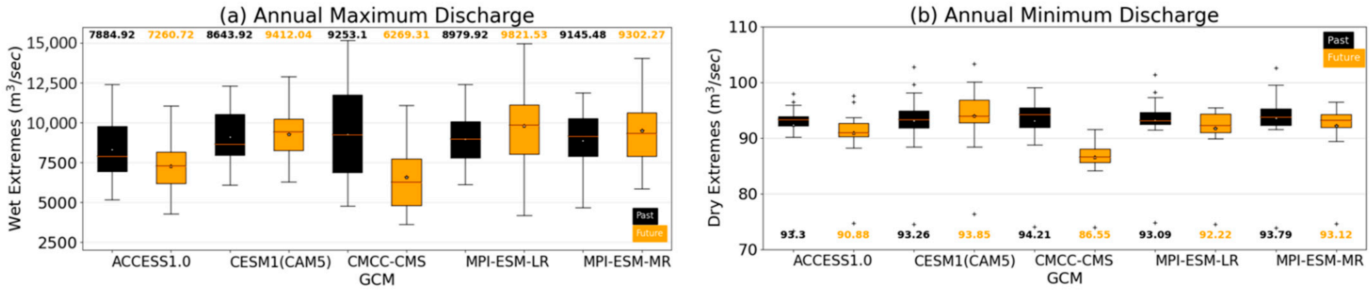

Figure 13. Wet and dry extreme discharge changes at the GERD dam using a box–whisker for annual maximum and minimum extreme records between future and past periods. The top bar is a maximum percentile, the lower bar is a minimum percentile, the top of the box is the third quartile, the bottom of the box is the first quartile, the middle bar in the box is the median value, plus sign represents the outlier, and the star sign within the box represents the mean value.

4. Discussion

This study evaluated the impact of climate change on future water resources and investigates climate-change-related uncertainties regarding the Blue Nile basin using 30 years of observed hydro-climatic data and statistically bias-corrected outputs of five GCMs selected based on their regional performance through DIAS-CMIP5 tools. The observed data show a monotonically increasing trend in temperature and extreme rainfall while the total precipitation shows an unsteady trend. The GCM projection under RCP8.5 scenarios provides evidence of uniformity in the temperature increase indicating an extremely likely warmer climate in the future. The climate projection also indicates a high probability that extremely dry and wet events will occur in the future period.

The analysis of total precipitation in GCMs indicates an increase in three of the five models (i.e., CESM1(CAM5), MPI-ESM-MR, and MPI-ESM-LR), while ACCESS1.0 remains the same and CMCC-CMS shows a decreasing trend. The seasonal precipitation projections indicated a difference from the annual, particularly in the rainy season. The Kiremt (JJAS) season was used to assess the uncertainties of projection as the bulk rainfall in the Blue Nile region is received in this season. Similarly, trends in observed precipitation were found to show seasonality, increasing in Kiremt and decreasing in Bega seasons. The spatial distribution at stations indicated the sensitivity of the southern part of the basin, particularly the Dedesa and Dabus sub-basins, to both increasing and decreasing trends. The results indicate high inter-annual and spatial variability in precipitation projection. While previous studies also indicated uncertainty in precipitation projection in the Nile region [11–15], this study investigated the sources of differences in the GCM's climate variables for understanding the variance in GCMs.

As a result, an uncertainty analysis of precipitation projection conducted in major climatic physical variables over a wider domain identifies wind vector dynamics as a key factor for the projected precipitation differences in GCMs. Meanwhile, no robust trend was found in the statistical comparison of geopotential height, specific humidity, outgoing longwave radiation, and sea surface pressure (SLP) in the synoptic scale. Studies show that Ethiopian rainfall is strongly influenced by Indian Ocean circulation and the ENSO [50,51].

The connection between Africa and India is also suggested to reflect a common imprint of the Madden–Julian oscillation, which is known to affect intra-seasonal variations of the Indian monsoon [52]. Moreover, a study on the CMIP5 GCM's climate projection indicates changes in the strengthening of Hadley Circulation in the deep tropics induce atmospheric moisture divergence and reduce tropospheric relative humidity, resulting in an increased frequency of dry events in preferred geographic locations worldwide [4]. In future studies, this can be addressed through a detailed assessment of climate variables at various pressure levels. The uncertainty analysis can also provide inputs for the improvement of climate model accuracy.

The analysis of river flow at selected locations from upstream to downstream indicates high variability in the projected changes and suggested a likely increase in flow discharge in the future. The flood inundation with an all-time peak inundation and the evapotranspiration comparison indicate a high likely increase in both parameters. The interconnectedness of changes in temperature, evapotranspiration, and water availability is also expected to affect agricultural productivity. Allam et al. [49] estimates the spatial and temporal distribution of ET in the Blue Nile basin and found that the actual ET exceeds the potential ET with a peak actual evapotranspiration rate of approximately 150 mm/month from July through September. Thus, it is very likely that flooding due to peak discharge and drought (resulting from extremely low flow) would increase in the future period. The comparative assessment of changes in observed trends and the results of GCM projections provided in this study enables a qualitative assessment (Table 4) with a high confidence level.

Table 4. Summary of basin-scale climate change assessment.

	Meteorological Assessment			**Hydrological Assessment**		
	Temperature	**Extreme Rainfall**	**Total Rainfall**	**Total Discharge**	**High Flow (Flood)**	**Low Flow (Drought)**
Level of confidence	Extremely likely increase	Very likely increase	Likely increase	Likely increase	Very likely increase	Very likely increase

Further, seasonal and extreme flow projections indicate a reduction in future low flow and an increase in high flow with high inter-annual variability, including a likely increase in the frequency of seasonal extreme inflows to the Grand Ethiopian Renaissance Dam (GERD). Although 85% of Nile waters originate in Ethiopia, nearly all related consumption occurs downstream in Egypt and Sudan, and the GERD operations are expected to significantly change downstream flow patterns [5,53]. The GERD dam, which is near completion, had three consecutive years of progressive storage (i.e., 2020 to 2022); however, the downstream area experienced devastating floods during these particular periods. As a result of this study, the frequency of the extreme flow to the GERD dam is found to increase even more. In light of this, the outputs of this study suggest operational considerations aimed at optimizing existing and proposed dams for water resource management and disaster risk reduction in addition to their intended purposes. If the GERD is properly operated, it would generate substantial economic benefits and enhance economic growth and welfare in all the Eastern Nile countries through basin-wide power trade [54]. To envision shared benefits and reimagine more prosperous development among the riparian countries, encouraging partnerships and moving beyond business-as-usual are indispensable. This study also suggests the vitalization of water infrastructure for basin-wide climate change adaptation based on scientific projections (e.g., GERD, Rosaries, and Sennar dams). This kind of activity will also reduce the cost inquired by loss and damages due to improper planning. Furthermore, the consideration of climate change risk in transboundary river negotiations and treaties can fundamentally enhance the equitable and reasonable use of water resources based on internationally available water laws, the UN Sustainable Development Goals (SDGs), and the general principles of the Sendai Framework for Disaster Risk Reduction.

5. Conclusions

This study applies a novel methodological approach to achieve findings helpful for a substantial understanding of the impact of climate change on the water resource of the Blue Nile basin. The meteorological assessment, temperature and precipitation, and the hydrological assessment of total and extreme flow provide evidence indicative of future extreme condition occurrence. The quantitative and qualitative results presented here indicate the need for the integration of future developments in climate change adaptation and disaster risk reduction in the Nile River basin. An increase in the frequency of extremely high flow with high inter-annual variability would pose flood hazards. Seasonally low flow reduction would affect agricultural productivity and environmental flow in the basin. As a result, the optimization of dam operation is recommended to reduce the impact of the inter-annual and spatial variability of dry and wet seasons, as well as extreme flood and drought events. In a transboundary context, the operation of water storage infrastructure in response to climate change scenarios would help countries to generate returns and improve their ability to cope with the risk of floods and droughts [5]. Flooding during peak flow and irrigation water release during low flow require operational adjustment to accommodate the total volume increase and seasonal fluctuation so as to smooth downstream release. Furthermore, the results indicate that the GERD dam offered an opportunity to maximize the availability of water for irrigation and environmental flow and mitigate flood and drought risks as an element of climate change adaptation. In addition, the GERD hydroelectric generation operation could enhance downstream water storage in locations including the high Aswan dam. Consequently, GERD dam operation could enhance disaster risk reduction, basin planning, and cooperation across the entire Nile River basin.

We conclude that the climate change assessment methodology developed in this study is a useful tool to transparently study climate change projection under uncertainty and could provide evidence that would support future efforts to adapt to climate change. These results also point to a need for research on the optimization of water storage system operation with climate change scenarios and research on topics including real-time monitoring for disaster risk reduction. The results presented here are clear and practical and include ways to formulate projections for addressing uncertainty in climate change. Addressing climate hazards, particularly in transboundary water systems under development, not only mitigate the water-related challenges but also provide an opportunity for consilience between researchers and the community in the form of informed decision-making and the implementation of Integrated Water Resource Management (IWRM). Furthermore, from this study, it is notable that directing efforts to climate change mitigation and adaptation through reducing emissions and cooperation is key to reducing loss and damages. Future directions of this research should focus on analyzing reservoir optimization and real-time monitoring under a changing climate in the Nile basin.

Author Contributions: Conceptualization, data curation, formal analysis, M.G.T.; funding acquisition, T.K.; methodology, M.G.T., H.S. and M.R.; project administration, M.R. and T.K.; resources, M.R. and K.T.; software, M.G.T. and M.R.; supervision and validation, M.R. and T.K.; visualization, M.G.T. and K.T.; writing—original draft, M.G.T.; writing—review and editing, M.R. and T.K. All authors have read and agreed to the published version of the manuscript.

Funding: This research received no external funding.

Institutional Review Board Statement: Not applicable.

Informed Consent Statement: Not applicable.

Data Availability Statement: All the GCM data used in this study are openly available in DIAS from https://diasjp.net/en/service/cmip5/ (accessed on 24 October 2021). Other data are also available from their sources that can be found in the data section.

Acknowledgments: This research is supported by the Public Work Research Institute (PWRI), Japan. CMIP5 data was collected and analysis tool was provided under the Data Integration and Analysis System (DIAS), which was developed and operated by the University of Tokyo and project supported by the MEXT, Japan. The authors would like to thank the Ethiopian National Meteorology Institute, the Ministry of Water and Energy, the Nile Basin Initiative, and NASA for providing data and resources for analysis and model simulations and evaluation. We thank Lawrie Hunter (Center for Professional Communication, GRIPS) for academic writing and editing support. We also acknowledge anonymous reviewers for their comments and suggestions that improved this manuscript.

Conflicts of Interest: The authors declare no conflict of interest.

References

1. *Climate Change 2007: The Physical Science Basis: Contribution of Working Group I to the Fourth Assessment Report of the Intergovernmental Panel on Climate Change*; Solomon, S.; Qin, D.; Manning, M.; Chen, Z.; Marquis, M.; Averyt, K.B.; Tignor, M.; Miller, H.L. (Eds.) Cambridge University Press: Cambridge, UK, 2007; p. 996.
2. Niang, I.; Ruppel, O.C.; Abdrabo, M.A.; Essel, A.; Lennard, C.; Padgham, J.; Urquhart, P.; Adelekan, I.; Archiblad, S.; Balinga, M.; et al. Chapter 22 Africa. In *Climate Change 2014: Impacts, Adaptation, and Vulnerability. Part B: Regional Aspects. Contribution of Working Group II to the Fifth Assessment Report of the Intergovernmental Panel on Climate Change*; Barros, V.R., Field, C.B., Dokken, D.J., Mastrandrea, M.D., Mach, K.J., Bilir, T.E., Chatterjee, M., Ebi, K.L., Estrada, Y.O., Genova, R.C., et al., Eds.; Cambridge University Press: Cambridge, UK, 2014; pp. 1199–1265.
3. Möbis, B.; Stevens, B. Factors controlling the position of the Intertropical Convergence Zone on an aquaplanet. *J. Adv. Model. Earth Syst.* **2012**, *4*, M00A04. [CrossRef]
4. Lau, W.K.M.; Kim, K.-M. Robust Hadley Circulation changes and increasing global dryness due to CO_2 warming from CMIP5 model projections. *Proc. Natl. Acad. Sci. USA* **2015**, *112*, 3630–3635. [CrossRef]
5. Wheeler, K.G.; Jeuland, M.; Hall, J.W.; Zagona, E.; Whittington, D. Understanding and managing new risks on the Nile with the Grand Ethiopian Renaissance Dam. *Nat. Commun.* **2020**, *11*, 1–9. [CrossRef] [PubMed]
6. Koike, T.; Koudelova, P.; Jaranilla-Sanchez, P.A.; Bhatti, A.M.; Nyunt, C.T.; Tamagawa, K. River management system development in Asia based on Data Integration and Analysis System (DIAS) under GEOSS. *Sci. China Earth Sci.* **2014**, *58*, 76–95. [CrossRef]
7. Goly, A.; Teegavarapu, R.S.V.; Mondal, A. Development and Evaluation of Statistical Downscaling Models for Monthly Precipitation. *Earth Interact.* **2014**, *18*, 1–28. [CrossRef]
8. Rasmy, M.; Koike, T.; Lawford, P.; Hara, M.; Fujita, M.; Kimura, F. Assessment of Future Water Resources in the Tone River Basin Using a Combined Dynamical-Statistical Downscaling Approach. *J. Jpn. Soc. Civ. Eng. Ser. B1 (Hydraulic Eng.)* **2015**, *71*, I_73–I_78. [CrossRef]
9. Hulme, M.; Doherty, R.; Ngara, T.; New, M.; Lister, D. African climate change: 1900–2100. *Clim. Res.* **2001**, *17*, 145–168. [CrossRef]
10. Albritton, D.L.; Barker, T.; Bashmakov, I.A.; Canziani, O.; Christ, R.; Cubasch, U.; Davidson, O.; Gitay, H.; Griggs, D.; Houghton, J.; et al. *Climate Change 2001: Synthesis Report*; Watson, R.T., Albritton, D.L., Barker, T., Bashmakov, I.A., Canziani, O., Christ, R., Cubasch, U., Davidson, O., Gitay, H., Griggs, D., et al., Eds.; Cambridge University Press: Cambridge, UK, 2001; p. 397.
11. Elshamy, M.E.; Seierstad, I.A.; Sorteberg, A. Impacts of climate change on Blue Nile flows using bias-corrected GCM scenarios. *Hydrol. Earth Syst. Sci.* **2009**, *13*, 551–565. [CrossRef]
12. Worqlul, A.W.; Dile, Y.T.; Ayana, E.K.; Jeong, J.; Adem, A.A.; Gerik, T. Impact of Climate Change on Streamflow Hydrology in Headwater Catchments of the Upper Blue Nile Basin, Ethiopia. *Water* **2018**, *10*, 120. [CrossRef]
13. Kiros, G.; Shetty, A.; Nandagiri, L. Analysis of variability and trends in rainfall over northern Ethiopia. *Arab. J. Geosci.* **2016**, *9*, 451. [CrossRef]
14. Taye, M.T.; Ntegeka, V.; Ogiramoi, N.P.; Willems, P. Assessment of climate change impact on hydrological extremes in two source regions of the Nile River Basin. *Hydrol. Earth Syst. Sci.* **2011**, *15*, 209–222. [CrossRef]
15. Alemayehu, A.; Bewket, W. Local spatiotemporal variability and trends in rainfall and temperature in the central highlands of Ethiopia. *Geogr. Ann. Ser. A, Phys. Geogr.* **2017**, *99*, 85–101. [CrossRef]
16. Beyene, T.; Lettenmaier, D.P.; Kabat, P. Hydrologic impacts of climate change on the Nile River Basin: Implications of the 2007 IPCC scenarios. *Clim. Chang.* **2009**, *100*, 433–461. [CrossRef]
17. Taye, M.T.; Willems, P. Influence of downscaling methods in projecting climate change impact on hydrological extremes of upper Blue Nile basin. *Hydrol. Earth Syst. Sci. Discuss.* **2013**, *10*, 7857–7896.
18. Ehret, U.; Zehe, E.; Wulfmeyer, V.; Warrach-Sagi, K.; Liebert, J. HESS Opinions Should we apply bias correction to global and regional climate model data? *Hydrol. Earth Syst. Sci.* **2012**, *16*, 3391–3404. [CrossRef]
19. Vaittinada Ayar, P.; Vrac, M.; Mailhot, A. Ensemble bias correction of climate simulations: Preserving internal variability. *Sci. Rep.* **2021**, *11*, 3098. [CrossRef]
20. Mekonnen, D.F.; Disse, M. Analyzing the future climate change of Upper Blue Nile River Basin using statistical down scaling techniques. *Hydrol. Earth Syst. Sci.* **2018**, *22*, 2391–2408. [CrossRef]
21. Fiseha, B.M.; Melesse, A.; Romano, E.; Volpi, E.; Fiori, A. Statistical downscaling of precipitation and temperature for the Upper Tiber Basin in Central Italy. *Int. J. Water Sci.* **2012**, *1*.
22. Hagemann, S.; Chen, C.; O Haerter, J.; Heinke, J.; Gerten, D.; Piani, C. Impact of a Statistical Bias Correction on the Projected Hydrological Changes Obtained from Three GCMs and Two Hydrology Models. *J. Hydrometeorol.* **2011**, *12*, 556–578. [CrossRef]

23. Piani, C.; Haerter, J.O.; Coppola, E. Statistical bias correction for daily precipitation in regional climate models over Europe. *Arch. Meteorol. Geophys. Bioclimatol. Ser. B* **2009**, *99*, 187–192. [CrossRef]
24. Nyunt, C.T.; Koike, T.; Yamamoto, A. Statistical bias correction for climate change impact on the basin scale precipitation in Sri Lanka, Philippines, Japan and Tunisia. *Hydrol. Earth Syst. Sci. Discuss.* **2016**, *27*, 1–32.
25. Tariku, T.B.; Gan, K.E.; Tan, X.; Gan, T.Y.; Shi, H.; Tilmant, A. Global warming impact to River Basin of Blue Nile and the optimum operation of its multi-reservoir system for hydropower production and irrigation. *Sci. Total Environ.* **2021**, *767*, 144863. [CrossRef] [PubMed]
26. Zappa, G.; Shepherd, T.G. Storylines of Atmospheric Circulation Change for European Regional Climate Impact Assessment. *J. Clim.* **2017**, *30*, 6561–6577. [CrossRef]
27. Fajardo, J.; Corcoran, D.; Roehrdanz, P.R.; Hannah, L.; Marquet, P.A. GCM compare R: A web application to assess differences and assist in the selection of general circulation models for climate change research. *Methods Ecol. Evol.* **2020**, *11*, 656–663. [CrossRef]
28. Kawasaki, A.; Yamamoto, A.; Koudelova, P.; Acierto, R.; Nemoto, T.; Kitsuregawa, M.; Koike, T. Data Integration and Analysis System (DIAS) Contributing to Climate Change Analysis and Disaster Risk Reduction. *Data Sci. J.* **2017**, *16*, 41. [CrossRef]
29. Bizuneh, B.B.; Moges, M.A.; Sinshaw, B.G.; Kerebih, M.S. SWAT and HBV models' response to streamflow estimation in the upper Blue Nile Basin, Ethiopia. *Water-Energy Nexus* **2021**, *4*, 41–53. [CrossRef]
30. Takele, G.S.; Gebre, G.S.; Gebremariam, A.G.; Engida, A.N. Hydrological modeling in the Upper Blue Nile basin using soil and water analysis tool (SWAT). *Model. Earth Syst. Environ.* **2021**, *8*, 277–292. [CrossRef]
31. Worku, G.; Teferi, E.; Bantider, A.; Dile, Y.T. Modelling hydrological processes under climate change scenarios in the Jemma sub-basin of upper Blue Nile Basin, Ethiopia. *Clim. Risk Manag.* **2021**, *31*, 100272. [CrossRef]
32. Selvarajah, H.; Koike, T.; Rasmy, M.; Tamakawa, K.; Yamamoto, A.; Kitsuregawa, M.; Zhou, L. Development of an Integrated Approach for the Assessment of Climate Change Impacts on the Hydro-Meteorological Characteristics of the Mahaweli River Basin, Sri Lanka. *Water* **2021**, *13*, 1218. [CrossRef]
33. United Nations Development Programme (UNDP). Sendai Framework for Disaster Risk Reduction (2015–2030). Available online: https://www.undp.org/myanmar/publications/sendai-framework-disaster-risk-reduction-2015-2030 (accessed on 15 October 2022).
34. United Nations Framework Convention on Climate Change (UNFCCC). Adoption of the Paris Agreement. 2015. Available online: https://unfccc.int/resource/docs/2015/cop21/eng/l09r01.pdf (accessed on 12 January 2019).
35. World Bank. *Africa Development Indicators 2006: From the World Bank Africa Database*; The World Bank: Washington, DC, USA, 2006.
36. Seleshi, Y.; Demaree, G.R. Rainfall Variability in the Ethiopian and Eritrean Highlands and its Links with the Southern Oscillation Index. *J. Biogeogr.* **1995**, *22*, 945–952. [CrossRef]
37. Sellers, P.J.; Randall, D.A.; Collatz, G.J.; Berry, J.A.; Field, C.B.; Dazlich, D.A.; Zhang, C.; Collelo, G.D.; Bounoua, L. A Revised Land Surface Parameterization (SiB2) for Atmospheric GCMS. Part I: Model Formulation. *J. Clim.* **1996**, *9*, 676–705. [CrossRef]
38. Tedla, M.; Cho, Y.; Jun, K. Flood Mapping from Dam Break Due to Peak Inflow: A Coupled Rainfall–Runoff and Hydraulic Models Approach. *Hydrology* **2021**, *8*, 89. [CrossRef]
39. Kobayashi, S.; Ota, Y.; Harada, Y.; Ebita, A.; Moriya, M.; Onoda, H.; Onogi, K.; Kamahori, H.; Kobayashi, C.; Endo, H.; et al. The JRA-55 Reanalysis: General Specifications and Basic Characteristics. *J. Meteorol. Soc. Jpn. Ser. II* **2015**, *93*, 5–48. [CrossRef]
40. Mann, H.B. Nonparametric tests against trend. *Econometrica* **1945**, *13*, 245–259. [CrossRef]
41. Kendall, M.G. Further Contributions to the Theory of Paired Comparisons. *Biometrics* **1955**, *11*, 43. [CrossRef]
42. Sen, P.K. Estimates of the Regression Coefficient Based on Kendall's Tau. *J. Am. Stat. Assoc.* **1968**, *63*, 1379–1389. [CrossRef]
43. Hamed, K.H.; Rao, A.R. A modified Mann-Kendall trend test for autocorrelated data. *J. Hydrol.* **1998**, *204*, 182–196. [CrossRef]
44. Intergovernmental Panel on Climate Change (IPCC). Summary for Policymakers. *Climate Change 2022: Mitigation of Climate Change. Contribution of Working Group III to the Sixth Assessment Report of the Intergovernmental Panel on Climate Change.* Available online: https://www.ipcc.ch/report/ar6/wg3/downloads/report/IPCC_AR6_WGIII_SPM.pdf (accessed on 1 November 2022).
45. Rasmy, M.; Sayama, T.; Koike, T. Development of water and energy Budget-based Rainfall-Runoff-Inundation model (WEB-RRI) and its verification in the Kalu and Mundeni River Basins, Sri Lanka. *J. Hydrol.* **2019**, *579*, 124163. [CrossRef]
46. Intergovernmental Panel on Climate Change (IPCC). *Climate Change 2014: Synthesis Report. Contribution of Working Groups I, II and III to the Fifth Assessment Report of the Intergovernmental Panel on Climate Change*; Core Writing Team, Pachauri, R.K., Meyer, L.A., Eds.; IPCC: Geneva, Switzerland, 2014.
47. van den Hurk, B.; van Oldenborgh, G.J.; Lenderink, G.; Hazeleger, W.; Haarsma, R.; de Vries, H. Drivers of mean climate change around the Netherlands derived from CMIP5. *Clim. Dyn.* **2014**, *42*, 1683–1697. [CrossRef]
48. Hwang, Y.-T.; Frierson, D.M.W. Link between the double-Intertropical Convergence Zone problem and cloud biases over the Southern Ocean. *Proc. Natl. Acad. Sci. USA* **2013**, *110*, 4935–4940. [CrossRef]
49. Allam, M.M.; Figueroa, A.J.; McLaughlin, D.B.; Eltahir, E.A.B. Estimation of evaporation over the upper Blue Nile basin by combining observations from satellites and river flow gauges. *Water Resour. Res.* **2016**, *52*, 644–659. [CrossRef]
50. Beltrando, G.; Camberlin, P. Interannual variability of rainfall in the eastern horn of Africa and indicators of atmospheric circulation. *Int. J. Clim.* **1993**, *13*, 533–546. [CrossRef]
51. Mwalichi, J.I. The characteristics of rainfall in Ethiopia and its relationship to El-Nino Southern Oscillation. In Proceedings of the First Technical Conference on Meteorological Research in Eastern and Southern Africa, Nairobi, Kenya, 6–9 January 1987.

52. Camberlin, P.; Fontaine, B.; Louvet, S.; Oettli, P.; Valimba, P. Climate Adjustments over Africa Accompanying the Indian Monsoon Onset. *J. Clim.* **2010**, *23*, 2047–2064. [CrossRef]
53. Basheer, M. Cooperative operation of the Grand Ethiopian Renaissance Dam reduces Nile riverine floods. *River Res. Appl.* **2021**, *37*, 805–814. [CrossRef]
54. Kahsay, T.N.; Kuik, O.; Brouwer, R.; van der Zaag, P. Estimation of the transboundary economic impacts of the Grand Ethiopia Renaissance Dam: A computable general equilibrium analysis. *Water Resour. Econ.* **2015**, *10*, 14–30. [CrossRef]